

## Article

# Statistical Indoor Exclusion Zone Analysis by Investigating Electromagnetic Fields inside a Nuclear Power Plant

Doyoung Jang <sup>1</sup>, Sangwoon Youn <sup>1</sup>, Jun-Yong Lee <sup>2</sup> and Hosung Choo <sup>1,\*</sup>

<sup>1</sup> School of Electronic and Electrical Engineering, Hongik University, Seoul 04066, Korea; dyjang1224@mail.hongik.ac.kr (D.J.); tirano88@mail.hongik.ac.kr (S.Y.)

<sup>2</sup> School of Computer Engineering, Hongik University, Seoul 04066, Korea; jlee@hongik.ac.kr

\* Correspondence: hschoo@hongik.ac.kr

**Featured Application:** This article is related to a statistical method to obtain the indoor exclusion zone for an actual nuclear power plant environment.

**Abstract:** This article investigates a statistical indoor exclusion zone (EZ) that can be efficiently applied to a nuclear power plant (NPP) by examining electromagnetic fields inside the actual NPP. To obtain the statistical indoor EZ, the indoor environment of the Korea Institute of Nuclear Safety (KINS) simulator room is modeled using the Wireless InSite commercial electromagnetic simulation software. The indoor space around the transmitting antenna is classified as multiple observation regions, and the EZ boundaries of each region are independently defined within each separate observation region. The EZ boundaries are then obtained using a margined regression model, which makes it possible to determine a reasonable boundary of the statistical indoor EZ. To validate the statistical indoor EZ, the received power inside the KINS simulator room is then measured, which agrees well with the simulated results. The results demonstrate that the proposed statistical indoor EZ can be properly obtained not only from the simulation data but also from the measurement data.

**Keywords:** electromagnetic field strength; exclusion zone; regression model; statistical method; nuclear facility regulation



**Citation:** Jang, D.; Youn, S.; Lee, J.-Y.; Choo, H. Statistical Indoor Exclusion Zone Analysis by Investigating Electromagnetic Fields inside a Nuclear Power Plant. *Appl. Sci.* **2021**, *11*, 4199. <https://doi.org/10.3390/app11094199>

Academic Editor: Ernesto Limiti

Received: 4 April 2021

Accepted: 3 May 2021

Published: 5 May 2021

**Publisher's Note:** MDPI stays neutral with regard to jurisdictional claims in published maps and institutional affiliations.



**Copyright:** © 2021 by the authors. Licensee MDPI, Basel, Switzerland. This article is an open access article distributed under the terms and conditions of the Creative Commons Attribution (CC BY) license (<https://creativecommons.org/licenses/by/4.0/>).

## 1. Introduction

Recently in nuclear power plants (NPPs), there have been an increasing number of attempts to replace wired systems with wireless communication systems, because wired monitoring systems that use complex and heavy wire cables have installation and maintenance drawbacks [1,2]. However, wireless systems emit electromagnetic fields for communication purposes, which can be a potential hazard to instrumentation and control (I&C) equipment in NPP. This is because electromagnetic fields exceeding the tolerable threshold may cause malfunctions of the I&C equipment. To protect the I&C equipment from these unpredictable electromagnetic fields, the I&C equipment must be safely placed outside the exclusion zone (EZ). A guideline for the EZ is introduced in *Regulatory Guide 1.180* [3], but as this assumes a free space environment, it may not be suitable for an actual NPP that includes many interior structures. Previous studies have investigated the indoor electromagnetic fields inside the NPP when arbitrary wireless devices are in operation [4–6], but there has been no detailed discussion on the EZ. In a recent study, the EZ for the actual indoor environment was examined [7,8], but it is very difficult to determine the boundary between the EZ and the safe zone because the indoor EZ boundary is very complicated and irregularly distributed, which makes it difficult to apply in practice. To obtain an EZ that can be used in practice, the boundary of the EZ should not be too complicated, so that the I&C equipment can be easily placed in the safe zone. In addition, the EZ needs to be extended into a 3D volume space, since the EZ in previous studies is limited to a 2D plane with a fixed height.

In this paper, we propose a statistical indoor EZ that can be efficiently applied to an NPP by investigating electromagnetic fields inside the actual NPP. The proposed indoor EZ has much simpler boundaries than those reported in [7,8], since the EZ is achieved using a statistical regression analysis for practical use in the NPP. This means that the proposed statistical EZ is more suitable for real NPPs than conventional methods that have a complicated boundary. To obtain the statistical indoor EZ, the indoor environment of the simulator room of the Korea Institute of Nuclear Safety (KINS) is modeled using the Wireless InSite commercial electromagnetic simulation software [9]. In this simulation model, the transmitting and receiving antennas use the measured radiation patterns of the dipole antenna in order to make the simulation results more consistent with the actual values. The received power at the receiving antenna, caused by the transmitting antenna of the wireless system, is analyzed in all classified indoor observation regions with a 30° angle range. The statistical regression model [10,11] is applied to each piece of data included in the observation region. The boundaries of the EZ for each observation region can be achieved using a calculated regression model. Then, the EZ is extended into a 3D volume space by investigating at various heights, which helps us to understand the EZ in a 3D environment. The statistical EZs in the NPP are then compared with those in a free space case. To verify the proposed method, the electromagnetic field strengths according to the azimuth angle and distance from each transmitting antenna are measured, and are confirmed to be in good agreement with the simulation results. The results demonstrate that the proposed statistical indoor EZ can be properly obtained not only from the simulation data but also from the measurement data.

## 2. Derivation and Analysis for Statistical Indoor EZ

Figure 1 presents the derivation process to obtain the statistical indoor EZ for an actual NPP environment by investigating electromagnetic fields using a statistical method. To examine the indoor electromagnetic fields, the transmitting antenna is placed in an arbitrary location, and the received power is observed in all indoor locations. The proposed statistical indoor EZ is achieved according to the following procedure: first, the indoor space around the transmitting antenna is classified into multiple observation regions. In Figure 1a,  $\phi_T$  is the azimuth angle around the transmitting antenna. At the same time, the indoor space around the transmitting antenna is divided into 12 regions (*Region n* from *Region 1* to *Region 12*), each with a 30° angle range. EZ boundaries of each region are independently defined within each separate observation region, and the detailed information of each region is listed in Table 1. Second, the received power (by half wavelength dipoles for Rx. and Tx. antennas) is obtained at as many locations as possible in each region, when the total radiated power of the transmitting antenna is assumed to be 1 W. The received power can be obtained through electromagnetic simulations using the modeled indoor NPP environment or by using actual measurements. Herein, each received power datum within each region is arranged according to the azimuth angle and distance from the transmitting antenna. For example, the obtained received power data in *Region n* tend to gradually decrease with distance, as shown in Figure 1b. Third, the regression model [10–14] ( $f_1$ ) is applied for this stored received power data, which helps us to observe the tendency of the received power according to the distance. The regression model ( $f_1$ ) is derived based on a quadratic function, as indicated by the solid line in Figure 1b. The received power typically decreases in inverse proportion to the square of the distance from the transmitting antenna. The quadratic regression model is a general method to fit the data with a curved distribution [12–14]. The quadratic regression model can be expressed as below:

$$f_1(d) = a_1 \cdot d^2 + a_2 \cdot d + a_3 \quad (1)$$

where  $d$  is the distance from the transmitting antenna, and  $a_1$ ,  $a_2$  and  $a_3$  are coefficients that best fit the received power data. However, using the obtained regression model is not suitable for the boundary of the statistical indoor EZ. This is because, when applying the general regression function ( $f_1$ ) to the statistical indoor EZ, there are too many locations

where the received power exceeds the allowable received power ( $-10.6$  dBm according to the *Regulatory Guide 1.180* [3,8]). Therefore, the margined regression model ( $f_2$ ), where 95% of the data lie below the curve, is defined based on the general regression model ( $f_1$ ), as shown by the dashed line in Figure 1b. The margined regression model ( $f_2$ ) can be defined as below:

$$f_2(d) = f_1(d) \cdot K \tag{2}$$

where  $K$  is the offset of the margined regression model, which makes it possible to determine a reasonable boundary of the statistical indoor EZ. Finally, the boundaries ( $d_n$ ) of each region (*Region n*) are determined by finding the intersection between the allowable received power ( $-10.6$  dBm) and the margined regression model, as indicated in Figure 1b. This distance  $d_n$  is the boundary of the statistical indoor EZ at the specific azimuth range (*Region n*). By using the proposed statistical indoor EZ, we can obtain a less complicated EZ that can be easily applied to the actual NPPs. Then, the I&C equipment can be intuitively placed outside the proposed indoor EZ to satisfy safety issues in accordance with *Regulatory Guide 1.180*.

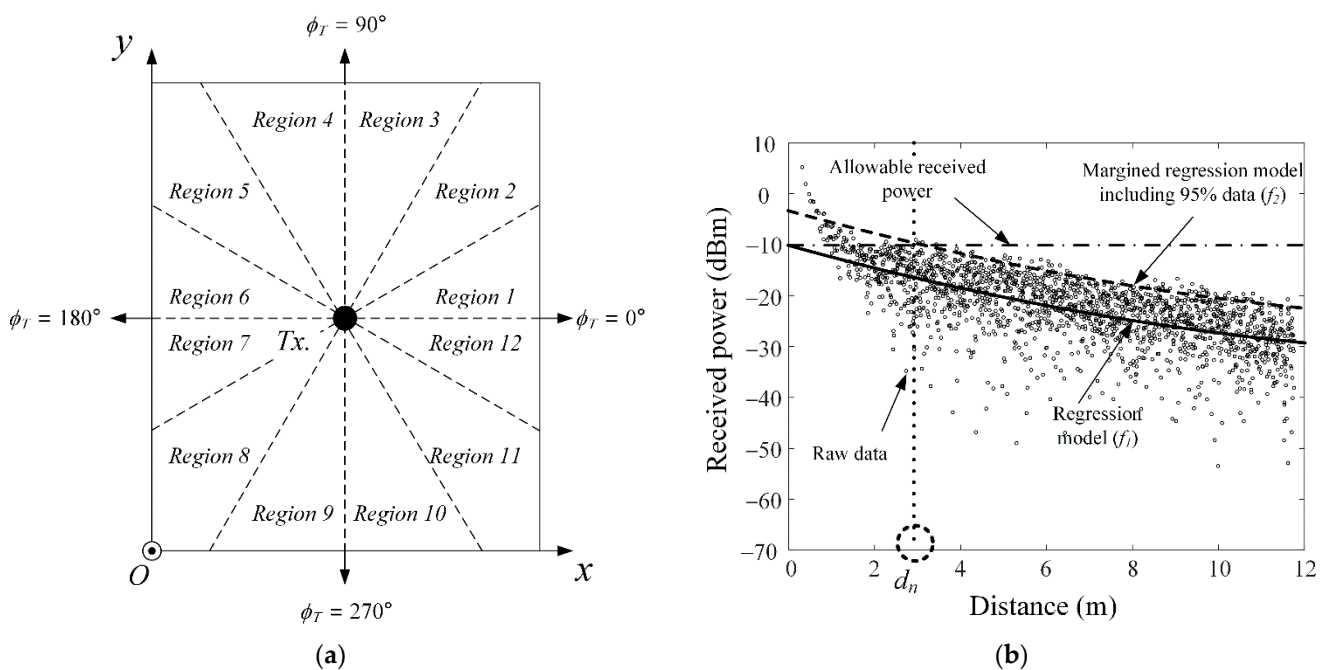


**Figure 1.** Process to obtain the statistical EZs based on electromagnetic field strengths in the indoor environment: (a) indoor regions; (b) acquisition of the statistical EZ boundary for *Region n*.

**Table 1.** Detailed information of all observation regions.

Regions According to Angle	Observation Angle Range
<i>Region 1</i>	$0^\circ < \phi_T < 30^\circ$
<i>Region 2</i>	$30^\circ < \phi_T < 60^\circ$
<i>Region 3</i>	$60^\circ < \phi_T < 90^\circ$
<i>Region 4</i>	$90^\circ < \phi_T < 120^\circ$
<i>Region 5</i>	$120^\circ < \phi_T < 150^\circ$
<i>Region 6</i>	$150^\circ < \phi_T < 180^\circ$
<i>Region 7</i>	$180^\circ < \phi_T < 210^\circ$
<i>Region 8</i>	$210^\circ < \phi_T < 240^\circ$
<i>Region 9</i>	$240^\circ < \phi_T < 270^\circ$
<i>Region 10</i>	$270^\circ < \phi_T < 300^\circ$
<i>Region 11</i>	$300^\circ < \phi_T < 330^\circ$
<i>Region 12</i>	$330^\circ < \phi_T < 360^\circ$

Figure 2 shows the photograph and geometry of the indoor environment of the simulator room of the KINS. The KINS simulator room is similar to the actual control room of the NPP, so it is suitable for examining the indoor electromagnetic fields of the NPP. To investigate the statistical indoor EZ, the indoor environment of the simulator room of KINS is modeled using Wireless InSite electromagnetic simulation software [9]. The entire simulator room has dimensions of 15 m × 18 m × 6 m. There are some interior structures (monitoring devices, control equipment, cabinets, and tables) in which the internal structures are typically made of metal or wood materials. In Figure 2b, the monitoring devices and control equipment are marked as A and C, while the metallic cabinet and the table are represented by B and E, respectively. D and G are wooden cabinets, and F is a wooden table. The coordinates of the transmitting antenna are denoted by  $x_t$  and  $y_t$ . The dimensions of all interior structures can also be represented by  $w$  m ×  $l$  m ×  $h$  m, where  $w$  and  $l$  are the width and length from the top view,  $h$  is the height, and  $t$  is the thickness of each interior structure. The detailed parameters of all modeled structures are listed in Table 2.

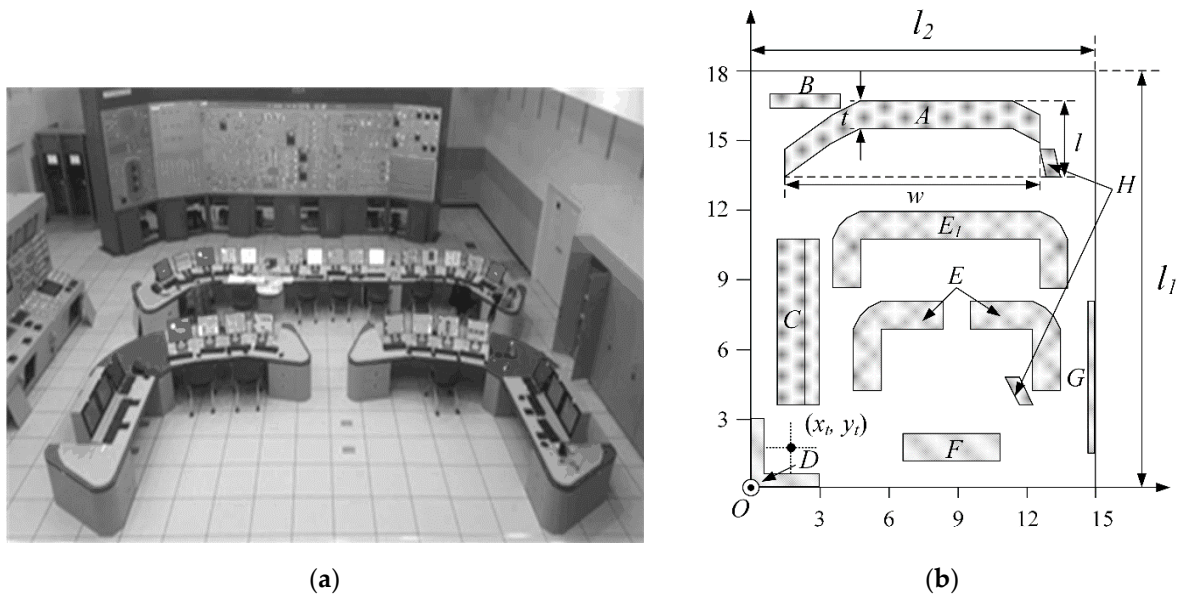


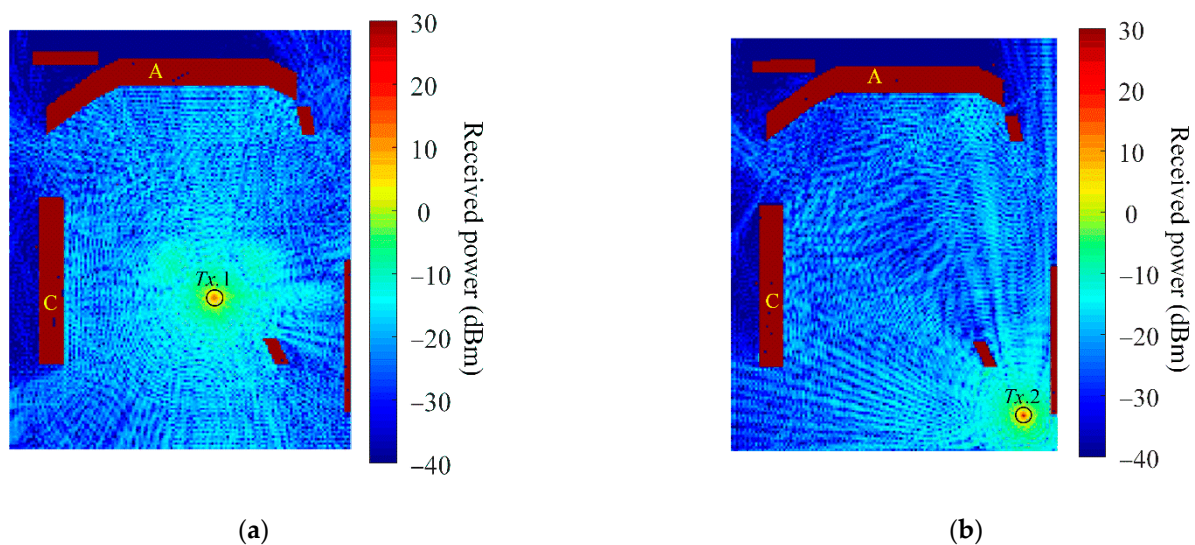
Figure 2. Photograph and geometry of the simulator room in KINS: (a) photograph; (b) geometry.

Table 2. Parameters of the structure in Figure 2b.

Symbols	$w$ (m)	$l$ (m)	$t$ (m)	$h$ (m)
A	11.2	3.3	1.2	3
B	3	0.6	-	2
C	1.8	7.2	-	2
D	3	3	0.5	1.2
E	3.8	3.8	1.2	0.8
$E_1$	10.2	3.2	1.2	0.8
F	4.2	1.2	-	0.8
G	0.3	6.6	-	2
H	0.9	1	0.6	1.5

Figure 3 illustrates the received power distributions according to the transmitting antenna position using Wireless InSite electromagnetic simulation software [9]. The total radiated power and frequency of the transmitting signal are assumed to be 1 W and 2.4 GHz, respectively. Herein, 2.4 GHz is used for observation, since the frequency band is used in various applications such as Bluetooth, Wi-Fi, and WirelessHART [15–17]. In order to make the simulation results more consistent with the actual values, the measured

radiation pattern of the dipole antenna (for transmitting and receiving antennas) is used as the input for the simulation. Detailed information of the fabricated dipole antenna will be introduced in Section 3. The position of  $Tx. 1$  is assumed at  $x_t = 9.5$  m and  $y_t = 6.5$  m. The height of the transmitting antenna is 1.4 m, which is higher than most interior structures in the simulator room. Therefore, the electromagnetic waves produced by the transmitting antenna propagate relatively evenly in all azimuth directions without significant interference from the interior structures as shown in Figure 3a. However, since the heights of equipment A and C are both above 2 m, there is a shaded area on the back of the equipment. On the other hand, when the transmitting antenna is located at  $Tx. 2$  ( $x_t = 13.5$  m and  $y_t = 1.5$  m), as shown in Figure 3b, the radiated electromagnetic fields are more affected by the indoor wall than in Figure 3a. Stronger electromagnetic fields are even observed around equipment A, which is further away from the transmitting antenna, due to the reflection effect caused by the wall.



**Figure 3.** Received power distribution according to transmitting antenna position: (a)  $Tx. 1$ ; (b)  $Tx. 2$ .

In Figure 4, the black line is the EZ assuming the NPP as free space, which is reported in *Regulatory Guide 1.180*. When the input power and the gain of the transmitting antenna are 1 W and 2.15 dBi, respectively, it has a circular shape with a radius of 1.75 m. On the other hand, the red line indicates the statistical indoor EZ boundary ( $d_n$ ) in terms of the azimuth angle regions (*Region n*) based on the environment in Figure 3 (the height of the receiving antenna ( $h_{rx}$ ) is 1.4 m). In contrast to the free space EZ, it can be seen that the EZ boundary ( $d_n$ ) differs depending on the directions of the azimuth angle. In Figure 4a, when the transmitting antenna is placed at  $Tx. 1$ , the EZ boundary ( $d_n$ ) in all regions is observed from a minimum of 2.8 m to a maximum of 7.4 m. The maximum of 7.4 m ( $d_4$ ) at *Region 4* ( $\phi_T = 90\sim 120^\circ$ ) is examined because of stronger electromagnetic fields due to the reflection by the equipment A. On the other hand, in *Region 12* ( $\phi = 330\sim 360^\circ$ ), there is no structure that generates strong reflections near the transmitting antenna in order for the distance ( $d_{12}$ ) of *Region 12* to be shorter than the distance ( $d_4$ ) of *Region 4*. In Figure 4b, the EZ boundary ( $d_n$ ) in all regions is observed from a minimum of 1.3 m (at *Region 1*) to a maximum of 11.7 m (at *Region 4*) when the transmitting antenna is located at  $Tx. 2$ . In this case, the electromagnetic field distribution is affected by equipment A as well as the indoor wall, and thus the maximum  $d_n$  is greater than in the case of Figure 4a. Additionally, to understand the EZ in a 3D environment, the EZ is extended into a 3D volume space by investigating at various heights. When the height of the receiving antenna ( $h_{rx}$ ) is 1.2 m, as shown by the blue line in Figure 4, the distance ( $d_7$ ) of *Region 7* is greater than the red line, because the wave reflected by structure D and F is stronger than when  $h_{rx}$  is 1.4 m. On the other hand, when  $h_{rx}$  is 1.6 m (the green line in Figure 4), the EZ boundary is much more

reduced than the red line. This is because, in the line-of-sight direction, both the influence of the structure and the antenna gain are reduced.

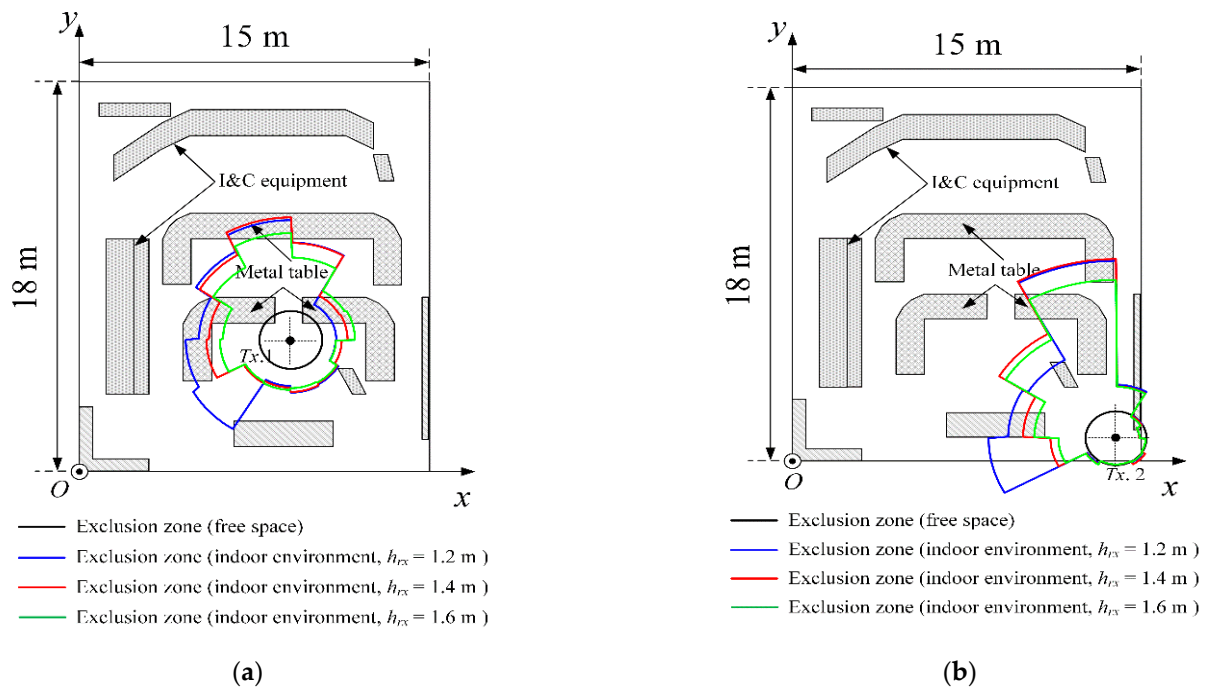


Figure 4. Comparisons of statistical indoor EZs according to transmitting antenna positions: (a) Tx. 1; (b) Tx. 2.

### 3. Measurement and Verifications

To verify the statistical indoor EZ in Section 2, we measured the received power inside the KINS simulator room using the test setup consisting of the dipole antennas, signal generator, power amplifier, and spectrum analyzer. Figure 5 shows the geometry and photograph of the dipole antenna for the received power measurement in the KINS simulator room. The dipole antenna consists of a balun which is embedded in the circuit board to minimize the pattern distortion by the unbalanced current of the coaxial feed. In addition, two metallic wires are connected to the balun through the circuit board with soldering, and each wire's length is 30 mm, as shown in Figure 5a. The fabricated dipole is presented in Figure 5b, which is fabricated as a pair for use as the transmitting and receiving antennas, respectively.

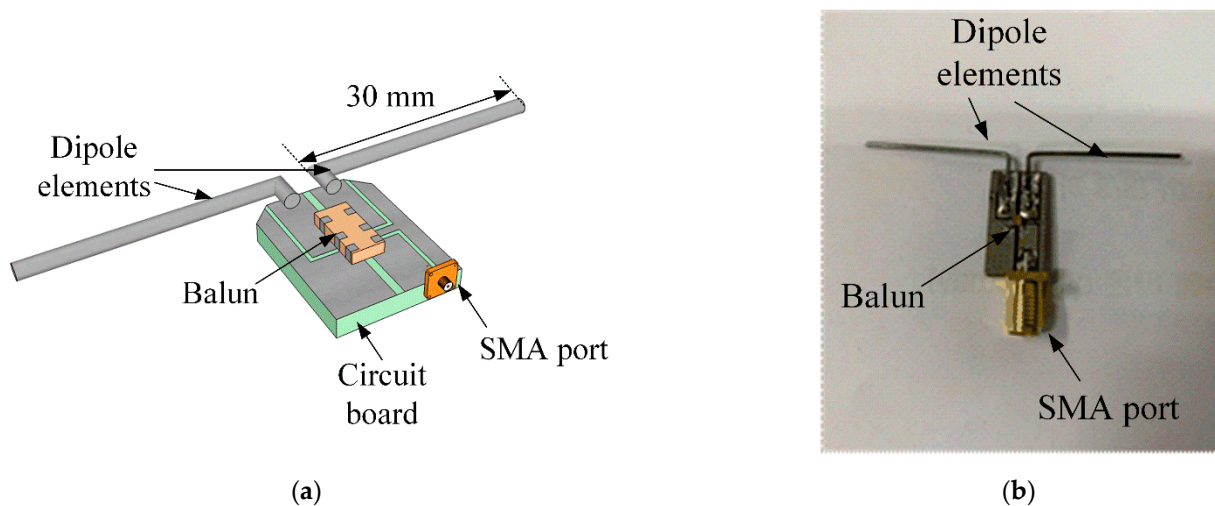
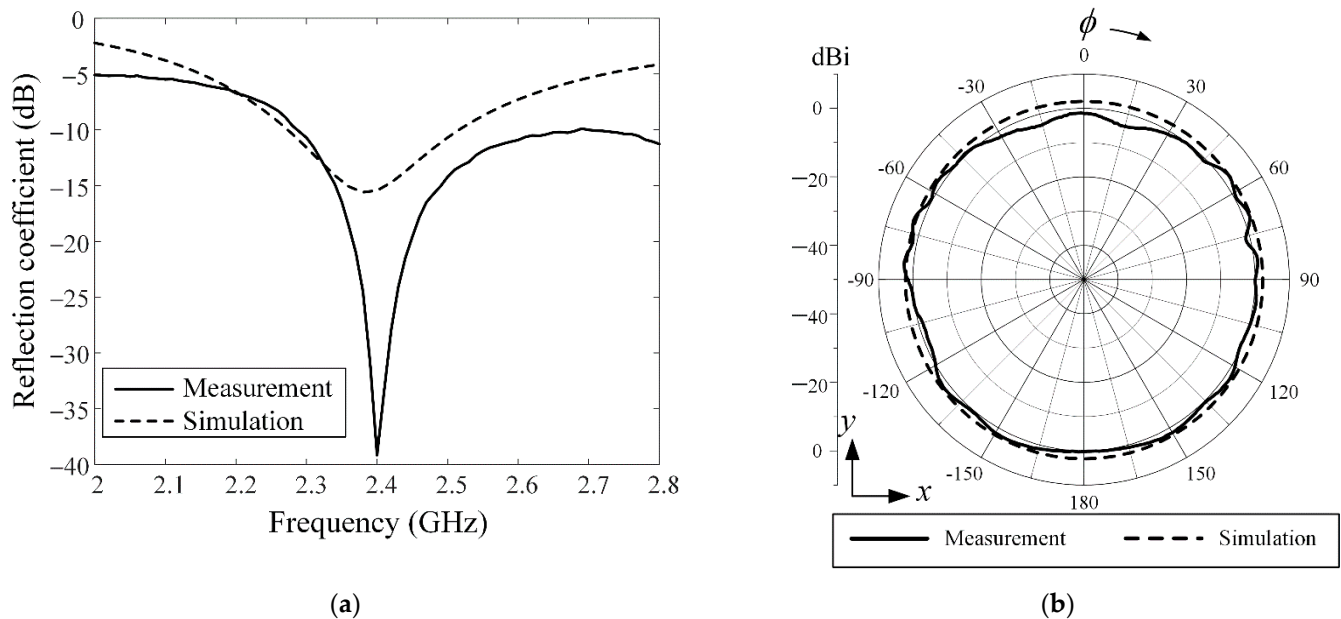


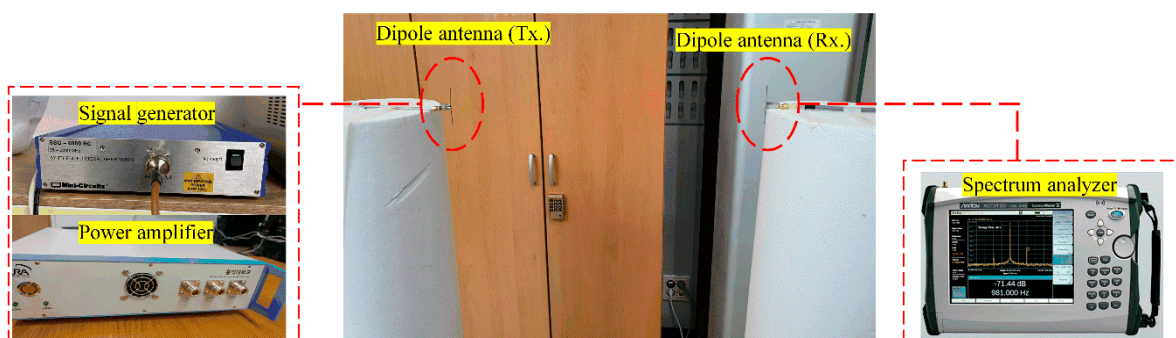
Figure 5. Geometry and photograph of the dipole antenna: (a) geometry; (b) photograph.

Figure 6 provides the reflection coefficients and radiation patterns of the dipole antenna. In Figure 6a, the solid line and the dashed line indicate the measured and simulated reflection coefficient, respectively. The measured and simulated reflection coefficients are  $-30$  dB and  $-17$  dB at 2.4 GHz, respectively, which show a low reflection characteristic of less than  $-10$  dB at the operating frequency. In Figure 6b, the measured radiation patterns have an omni-directional property with an average gain of around 0 dBi in the azimuth plane, which is suitable for use as a probe capable of measuring the received power in all directions.



**Figure 6.** Reflection coefficients and radiation patterns of the dipole antenna: (a) reflection coefficient; (b) radiation pattern.

Figure 7 shows the test setup for measuring the indoor received power. In the test setup, the signal generator capable of creating electromagnetic waves at 2.4 GHz is employed. However, the signal generator does not have enough power to transmit the signal to a faraway receiving antenna. Therefore, the output power (0 dBm) of the signal generator is amplified through a power amplifier with a gain of 30 dB. Then, the input power of 1 W (30 dBm) is finally delivered to the transmitting dipole antenna. Herein, the amplified signal is radiated through the transmitting dipole antenna, and, simultaneously, the spectrum analyzer with the receiving dipole antenna observes the received power.



**Figure 7.** Test setup for the indoor received power measurement.

Figure 8 presents the comparison of the measured and simulated received power according to the distance between the transmitting and receiving antenna when the transmitting antenna is placed at  $Tx. 2$ . The blue 'x' markers indicate the measured data, and the

black ‘o’ markers are the simulated data. The received power is measured at 60 cm intervals according to the distance from the transmitting antenna ( $T_x$ . 2), and it is examined for two regions of *Region 3* (Figure 8a) and *Region 7* (Figure 8b). In Figure 8a, the measured received power has a distribution range from  $-23.5$  dBm to  $-7$  dBm, which agrees well with the simulated data. The measured received power in Figure 8b is distributed from  $-31.5$  dBm to  $-8.5$  dBm. The results demonstrate that the proposed statistical indoor EZ can be properly obtained not only from the simulation data but also from the measurement data.

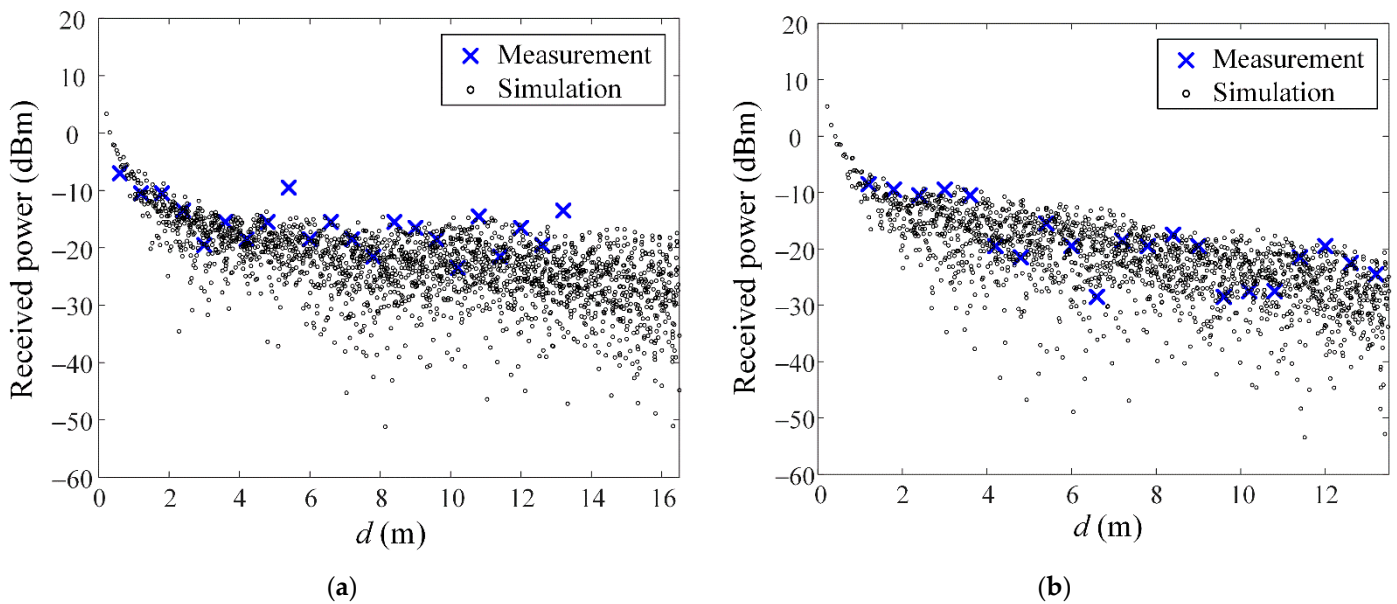


**Figure 8.** Comparison of measured and simulated received power when the transmitting antenna is placed at  $T_x$ . 2: (a) *Region 3*; (b) *Region 7*.

Figure 9 presents an RMSE according to the sampling interval, which can explain how many samples are needed to provide a reliable estimation of the EZ. To obtain this result, we adjusted the sampling interval from 0.1 m to 0.9 m based on the simulation results, where the area of the EZ is calculated for each case. Herein, RMSE is obtained by examining the EZ area difference between the case of Figure 4 (sampling interval of 0.1 m) and other cases (sampling interval from 0.2 to 0.9 m). The RMSE significantly decreases under 1.6 when the sampling interval is less than 0.6 m.

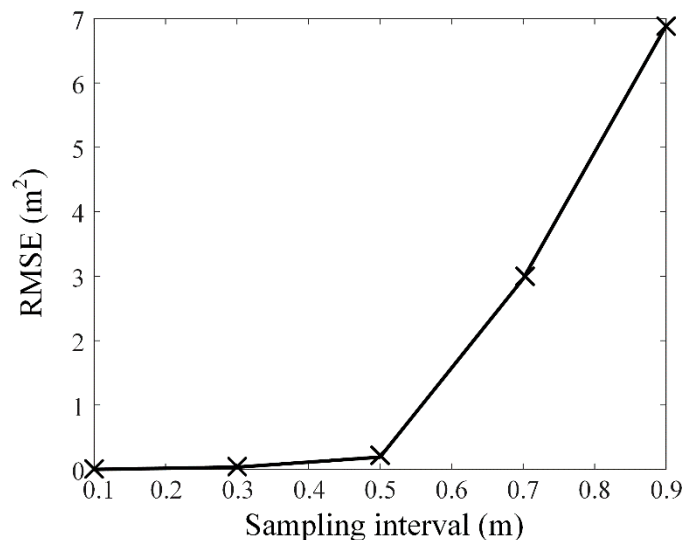


**Figure 9.** Comparison of RMSE according to sampling intervals.

#### 4. Conclusions

We have investigated the statistical indoor EZ that can be efficiently applied to an NPP by investigating electromagnetic fields inside the actual NPP. To obtain the statistical indoor EZ, the indoor environment of the KINS simulator room was modeled. In this simulation model, both the transmitting and receiving antenna used a measured radiation pattern of the dipole antenna to make the simulation results more consistent with the actual values. The indoor space around the transmitting antenna was classified as multiple observation regions, and the EZ boundaries of each region were independently defined within each separate observation region. The EZ boundaries were obtained using a margined regression model that included 95% of the data that were defined based on the general regression model, which can determine a reasonable boundary of the statistical indoor EZ. The EZ boundary in all regions was observed from the minimum of 2.8 m to the maximum of 7.4 m when the transmitting antenna was placed at *Tx. 1* (near the center of the room), and the height of the receiving antenna was 1.4 m. On the other hand, when the transmitting antenna was located in *Tx. 2* (the corner of the room), the distance between the transmitting antenna and the EZ boundary ranged from a minimum of 1.3 m to a maximum of 11.7 m. Additionally, to understand the EZ in a 3D environment, the EZ was extended into a 3D volume space by investigating at various heights. To validate the statistical indoor EZ, we measured the received power inside the KINS simulator room when the transmitting antenna was placed at *Tx. 2*. The measured received power according to the distance between the transmitting and receiving antenna was observed to have a distribution range from  $-23.5$  dBm to  $-7$  dBm in *Region 3* and from  $-31.5$  dBm to  $-8.5$  dBm in *Region 7*. The measured received power agreed well with the simulated result. The results demonstrated that the proposed statistical indoor EZ can be properly obtained not only from the simulation data but also from the measurement data, and, therefore, the I&C equipment can be easily placed in the safe zone without complication.

**Author Contributions:** Conceptualization, D.J., S.Y., J.-Y.L. and H.C.; formal analysis, D.J. and S.Y.; funding acquisition, H.C.; investigation, D.J. and S.Y.; methodology, D.J. and S.Y.; project administration, H.C.; software, D.J.; supervision, H.C.; validation, D.J., S.Y., J.-Y.L. and H.C.; visualization, D.J.; writing—original draft, D.J. and S.Y.; writing—review and editing, D.J. and H.C. All authors have read and agreed to the published version of the manuscript.

**Funding:** This research received no external funding.

**Institutional Review Board Statement:** Not applicable.

**Informed Consent Statement:** Not applicable.

**Data Availability Statement:** Not applicable.

**Acknowledgments:** This work was supported by the Basic Science Research Program through the National Research Foundation of Korea (NRF) funded by the Ministry of Education (No. NRF-2017R1A5A1015596) and the NRF grant funded by the Korean government (No.2015R1A6A1A03031833; NRF-2017R1D1A1B04031890).

**Conflicts of Interest:** The authors declare no conflict of interest.

#### References

1. Keebler, P.F.; Berger, H.S. *Managing the Use of Wireless Devices in Nuclear Power Plants*; IN Compliance: Edina, MN, USA, 2011.
2. Agarwal, V.; Buttles, J.W.; Beaty, L.H.; Naser, J.; Hallbert, B.P. Wireless online position monitoring of manual valve types for plant configuration management in nuclear power plants. *IEEE Sens. J.* **2017**, *17*, 311–322. [[CrossRef](#)]
3. *Guidelines for Evaluating Electromagnetic and Radio-Frequency Interference in Safety-Related Instrumentation*; Regulatory Guide 1.180; U.S. Nuclear Regulatory Commission: Rockville, MD, USA, 2003.
4. Ko, D.Y.; LEE, S.I. Applicable approach of the wireless technology for Korean nuclear power plants. *Nucl. Eng. Des.* **2013**, *265*, 519–525. [[CrossRef](#)]
5. Israel, A.A.-S.; Roberto, L.-M.; Luis, H.H.-G.; Yunuén, L.-G.; Alejandra, A.-M.; Laura, G.C.-F.; Luis, A.A.-M. Review of electromagnetic compatibility on digital systems of nuclear power plants. *Eng. Des. Appl.* **2020**, *124*, 103–113.

6. Ye, S.-H.; Kim, Y.-S.; Lyon, M.-S. Verification of electromagnetic effects from wireless devices in operating nuclear power plants. *Nucl. Eng. Technol.* **2015**, *47*, 729–737. [[CrossRef](#)]
7. Park, J.-E.; Youn, S.; Choo, J.; Choo, H. Indoor exclusion zone analysis in a nuclear power plant with wirelessHART application. *IEICE Electron. Express* **2019**, *16*, 20190204. [[CrossRef](#)]
8. Jang, D.; Youn, S.; Park, J.-E.; Choo, J.; Choo, H. Electromagnetic field propagation and indoor exclusion zone analysis in a nuclear power plant. *IEEE Trans. Electromagn. Compat.* **2020**, *62*, 2386–2393. [[CrossRef](#)]
9. Remcom: Wireless InSite. [Online]. Available online: <http://www.remcom.com/wireless-insite> (accessed on 1 April 2021).
10. Li, S.; Ajarapu, V.; Djukanovic, M. Adaptive online monitoring of voltage stability margin via local regression. *IEEE Trans. Power Syst.* **2018**, *33*, 701–713. [[CrossRef](#)]
11. Rastogi, R.; Anand, P.; Chandra, S. Large-margin distribution machine-based regression. *Neural Comput. Appl.* **2020**, *32*, 3633–3648. [[CrossRef](#)]
12. Hajibabaei, D.; Ahmadi, A. Government Size and Human Development: Quadratic Regression Approach. *Int. J. Acad. Res. Bus. Soc. Sci.* **2014**, *4*, 160–166. [[CrossRef](#)]
13. Gregg, J.S.; Wyatt, F.B.; Kilgore, J.L. Determination of ventilatory threshold through quadratic regression analysis. *J. Strength Cond. Res.* **2010**, *24*, 2512–2515. [[CrossRef](#)] [[PubMed](#)]
14. Bachmaier, M. A confidence set for that x-coordinate where a quadratic regression model has a given gradient. *Stat. Pap.* **2009**, *50*, 649–660. [[CrossRef](#)]
15. Dhirgham, K.N. Miniature slotted semi-circular dual-band antenna for WiMAX and WLAN applications. *J. Electromagn. Eng. Sci.* **2020**, *20*, 115–124.
16. Sulakshana, C.; Srividya, G. A wide dual-band metamaterial-loaded antenna for wireless applications. *J. Electromagn. Eng. Sci.* **2020**, *20*, 23–30.
17. Industrial Networks—Wireless Communication Network and Communication Profiles—WirelessHART. IEC 62591. Available online: <https://webstore.iec.ch/publication/24433> (accessed on 1 April 2021).